

A. Murari, W. Arter, D. Mazon, M. Gelfusa, V. Ferat
and JET EFDA contributors

Symmetry Based Analysis of Macroscopic Instabilities in Thermonuclear Plasmas

“This document is intended for publication in the open literature. It is made available on the understanding that it may not be further circulated and extracts or references may not be published prior to publication of the original when applicable, or without the consent of the Publications Officer, EFDA, Culham Science Centre, Abingdon, Oxon, OX14 3DB, UK.”

“Enquiries about Copyright and reproduction should be addressed to the Publications Officer, EFDA, Culham Science Centre, Abingdon, Oxon, OX14 3DB, UK.”

The contents of this preprint and all other JET EFDA Preprints and Conference Papers are available to view online free at www.iop.org/Jet. This site has full search facilities and e-mail alert options. The diagrams contained within the PDFs on this site are hyperlinked from the year 1996 onwards.

Symmetry Based Analysis of Macroscopic Instabilities in Thermonuclear Plasmas

A. Murari¹, W. Arter², D. Mazon³, M. Gelfusa⁴, V. Ferat⁵
and JET EFDA contributors*

JET-EFDA, Culham Science Centre, OX14 3DB, Abingdon, UK

¹*Associazione EURATOM-ENEA per la Fusione, Consorzio RFX, 4-35127 Padova, Italy*

²*EURATOM-CCFE Fusion Association, Culham Science Centre, OX14 3DB, Abingdon, OXON, UK*

³*Association EURATOM-CEA, CEA Cadarache, 13108 Saint-Paul-lez-Durance, France*

⁴*Associazione EURATOM-ENEA - University of Rome "Tor Vergata", Roma Italy*

⁵*Arts et Métiers ParisTech Engineering College (ENSAM) 75013 Paris.*

** See annex of F. Romanelli et al, "Overview of JET Results",
(23rd IAEA Fusion Energy Conference, Daejeon, Republic of Korea (2010)).*

ABSTRACT.

By imposing symmetry constraints on basic types of bifurcations, equations that properly reproduce the behaviour of the most important instabilities in magnetically confined plasmas are derived. The predictions of these equations are consistent with the results of Tokamak experiments, indicating excellent prospects for the use of equivariant bifurcation theory to interpret the physics of high temperature laboratory plasmas, to forecast and control their macroscopic behaviour and to process the signals of their diagnostics.

1. THE SYMMETRIES OF THE TOKAMAK CONFIGURATION.

The best performing and most widely studied magnetic fusion configuration is the Tokamak [1]. Notwithstanding significant effort during the last decades, many aspects even of the large scale behaviour of the configuration are still poorly understood. Tokamak reactor relevant, high temperature plasmas are affected by a series of macroscopic and microscopic instabilities, which can have a significant impact on their performance. In addition to the often nonlinear interactions between these instabilities, the wide range of spatial and time scales involved render simulation of these plasmas a conceptually delicate and computationally demanding task. Moreover, very often both theories and simulations are developed in simplified geometries, assuming that the main macroscopic symmetries do not play a significant role in determining the final results. On the other hand, the Tokamak configuration is characterised by global symmetries, already presented using the formalism of group theory in [2]. A sufficiently realistic geometry for the present investigation of Tokamak plasmas is the periodic cylinder, which consists of a circular cylinder whose flat ends are identified with each other. This geometrical configuration is designed to approximate a large aspect ratio torus, i.e. a torus with the major radius much larger than the minor radius. The symmetries of this configuration consist first of all of two $SO(2)$ subgroups, corresponding to rotations in the two angular coordinates θ and ϕ (see figure 1). The remaining symmetry is a reflection symmetry $(\theta, \phi) \rightarrow (-\theta, -\phi)$, which can be understood considering that single fluid magnetohydrodynamics (MHD), the basic theory to model magnetised plasmas, is invariant under change of sign of the magnetic field. In this letter, the aforementioned symmetries are used to constrain the form of simple bifurcation equations to reproduce the behaviour of the most relevant macroscopic instabilities of the Tokamak configuration, sawteeth and Edge Localised Modes (ELMs).

2. EQUIVARIANT BIFURCATION THEORY AND TOKAMAK MAGNETOHYDRODYNAMIC MODELLING.

Bifurcation theory studies nonlinear systems in the regions of the parameter space in which their behaviour shows qualitative changes. The main idea is that, close to the bifurcation points, the system behaviour can be modelled by a small number of coupled Ordinary Differential Equations (ODEs), with the nonlinear interactions among the variables expressible by low order terms in Taylor expansions. Equivariant bifurcation theory [3] is the study of the effects of symmetry

constraints on the construction of such ODE systems. Equivariant bifurcation theory is therefore an appropriate framework for the investigation of the onset of nonlinear instabilities in complex systems such as Tokamaks. The main instabilities have been properly modelled by two nonlinear coupled equations, derived using equivariant bifurcation theory to impose the proper symmetry constraints as described in [2]. To quickly summarise the derivation of the two equations, one can start by writing a generic instability as

$$y = a \exp(in\phi) + \bar{a} \exp(-in\phi) \quad (1)$$

In relation (1), n is the integer mode number, a the time dependent mode amplitude and the overbar denotes the complex conjugate. Assuming that the dynamics of the mode $y(t)$ is Hamiltonian, upon imposing invariance under rotation to the axisymmetry breaking instability $y(t)$, the governing equation for a to cubic accuracy is of the form:

$$\ddot{a} = \gamma a + 2 a^3 \quad (2)$$

The interaction with an axisymmetric mode representing the tokamak equilibrium configuration will have to be via a term proportional to a^2 in order to satisfy equivariance [2]. Provided the axisymmetric mode is governed by dissipative dynamics, the simplest bifurcation model is the fold, which, once the interaction term is added, reads:

$$\dot{b} = \alpha - \beta b^2 - (\delta b + 1) a^2 \quad (3)$$

Relations (2) and (3) constitute the simplest set of coupled nonlinear equations, respecting the symmetries and which might fit the experimental signals. They are used in the rest of this letter to reproduce the sawteeth and ELM instabilities in data from JET (Joint European Torus) experiments (JET has major radius $R \approx 3\text{m}$ and minor radius $a \approx 1\text{m}$).

3. REPRODUCTION OF SAWTEETH BEHAVIOUR

One of the main macroscopic modes in a Tokamak is the sawtooth instability [4, 1], which is present over a wide range of operating conditions. This is observed as a relaxation oscillation in the centre of the plasma, which appears most clearly in the time evolution of the electron temperature and density but also of other quantities. In the case of the temperature, the clear signature is sawtooth-like behaviour of the time series waveform in the central region of the plasma, with inverted behaviour in the outer region. The abrupt collapse of the temperature is attributed to an $m = 1, n = 1$ instability in the centre (m is the poloidal mode number and n the toroidal mode number), which causes the expulsions of particles and energy detected as a heat pulse propagating in the outer region.

Figure 2 shows how this behaviour can be accounted for by the coupled equations (2) and (3). The

analysis has been made at three different radii: the centre of the plasma, where the dynamics consists of a slow rise followed by a sudden crash, and two more external radii, which are characterised by a quick rise, due to the heat pulse, followed by a slower decay. The main parameter governing the form of the individual spikes, sawtooth type bursts or propagating heat pulses, is δ . For $\delta < -0.04$ the sawtooth type behaviour of the green curve in figure 2 is obtained; for $\delta > -0.04$ one gets the propagating pulse shape of the red and blue curves in figure 2.

The time evolution of b does not only reproduce the behaviour of the sawteeth qualitatively but can also fit the experimental dynamic quantities quantitatively. This is shown in figure 3, in which the electron temperature evolution, derived from the Electron Cyclotron Emission on JET, is well reproduced by b . A few comments are in order. First of all, the evolution of b reproduces very well the electron temperature at all the radii for which the signal-to-noise ratio of the measurements is acceptable. The main reason behind the choice of the discharge shown is exactly the large amplitude of the sawteeth in the centre, which produces a significant heat pulse, whose propagation can be followed to the periphery of the plasma. In any case, it has been checked that the proposed set of two coupled equations can properly model also smaller and more regular sawteeth without any difficulty (in a certain sense the example shown is extreme compared to more usual sawteeth). The fact that the discharge reported does not reach a completely steady state, as can be seen by the fact that the sawteeth frequency is not constant, means that one is obliged to adjust the parameters of the equations for each time interval, shown in figure 3 using different colours. Even though this has required some effort, the result proves the flexibility and wide applicability of equations (2) and (3).

Moreover, the fitting of frequency can be justified by noticing that tiny perturbations of equation (2) may make a large change to the timescale of oscillations. This may be demonstrated by integrating (2) with respect to time once, giving

$$\dot{a}^2 = 2H + \gamma a^2 + a^4 \quad (4)$$

where H is a constant of integration which is determined by the values of a and \dot{a} at time t_0 ,

$$H = \frac{1}{2} (\dot{a}^2 - \gamma a^2 - a^4)_{t=t_0} \quad (5)$$

It can be shown that (2) is soluble in terms of elliptic functions that have amplitude C and period P , where $C^2 = \gamma[1+(1+8h)^{1/2}]/(-2\mu)$, $h = (-\mu)H/\gamma^2$ and

$$P \sim \frac{1}{2\sqrt{\gamma}} \ln \left(\frac{8}{h} \right) \text{ as } h \rightarrow 0 \quad (6)$$

provided $\mu < 0$ and $H > 0$. Hence, thanks to the logarithm in Eq. (6), a tiny change to a small value of H may change the period of nonlinear oscillation drastically without greatly affecting the amplitude.

The model economically explains, in terms of small perturbations at critical times, why the periods of both sawteeth and ELMs can vary significantly during a discharge,

A more problematic issue is the identification of the experimental quantity corresponding to a . It is remarked that the evolution of b can be made to fit the experimental value of the electron temperature or equivalent dynamic quantities, such as the SXR, with a theoretical a , obtained by setting the parameters of equation (2) to give the experimental period of the oscillations. There is quite possibly no single, experimentally measured quantity corresponding to the oscillation about the equilibrium represented by equation (2). Nonetheless, it has been verified that, in the magnetic signals, there are components oscillating at the same frequency of the sawteeth and that they can be properly fitted using equation (2). An example is shown in figure 4 for the same shot as in figure 3.

4. REPRODUCTION OF EDGE LOCALISED MODES

In the ASDEX device it was discovered in 1982 that, increasing sufficiently the input power, the plasmas tended to transit spontaneously to an enhanced confinement mode called the High confinement or H-mode [5]. The H-mode is characterized by the presence of a thin region of very low transport situated at the edge of the plasma. Steep gradients in the density and temperature profiles are observed across this region, called also the edge barrier. The H-mode is characterised by short bursts of another major instability, the ELM [6]. Each burst results in a significant decrease in the density and temperature of the plasma edge, mainly reducing the gradients of the edge barrier. The signature of the ELMs is very clear in the magnetic signals, in the diagnostic measuring the parameters of the electron fluid at the edge and in the D_α emission. Figure 5 shows how the time evolution of a sequence of ELMs, as seen in the magnetic coils, can be properly fitted by the system of coupled equations (2) and (3). Even in this case, the coupled equations can be adjusted so that $b(t)$ can closely reproduce the signal of the pick-up coils, which are considered the most direct measurements of the ELM instability.

CONCLUSIONS

The results reported in this letter show for the first time that the system of coupled nonlinear equations (2) and (3) can reproduce very well the behaviour of the two most important macroscopic instabilities affecting Tokamak plasmas: sawteeth and ELMs. This fact has been proven using data of the most advanced Tokamak in operation: JET. From a practical point of view, the availability of robust, simple equations, capable of reproducing the salient features of the major plasma instabilities, could be very valuable for real time control. Such systems of equations could be used in model based control strategies, for advanced forecasting, in signal processing and advanced data assimilation schemes (the Kalman filter for example).

The reported evidence indicates that the symmetries of the magnetic configurations can play a significant role in determining the dynamics of the plasma, and lends force to the idea that the technique should also be applied to the reversed field pinch and stellarator magnetic fusion devices.

In the particular case of the Tokamak, since the two equations (2) and (3) have been derived by imposing geometrical symmetries and ideal MHD constraints, there is now a clear expectation that MHD theory is the right framework to investigate the gross behaviour of the sawteeth and ELM instabilities [7]. Moreover, our results motivate future investigations, which will see the same approach applied to the study of the third major nonlinear phenomenon in Tokamaks: disruptions.

ACKNOWLEDGMENTS

This work, supported by the European Communities under the contract of Association between EURATOM/ENEA, CCFE and CEA, was carried out under the framework of the European Fusion Development Agreement. The views and opinions expressed herein do not necessarily reflect those of the European Commission.

REFERENCES

- [1]. J. Wesson, *Tokamaks*. Oxford: Clarendon Press Oxford, 2004, Third edition.
- [2]. W. Arter, *Physical Review Letters* **102** (19):195004 (2009).
- [3]. R.B. Hoyle, *Pattern Formation: An Introduction to Methods*, Cambridge University Press, 2006.
- [4]. S. von Goeler, W. Stodiek and N. Sauthoff *Physical Review Letters* **33**, 1201 (1974).
- [5]. F. Wagner et al., *Physical Review Letters* **49**, 1408 (1982).
- [6]. ASDEX Team, *Nuclear Fusion* **29**, 1959 (1989).
- [7]. I.T. Chapman et al, *Physical Review Letter* **105**, 255002 (2010)

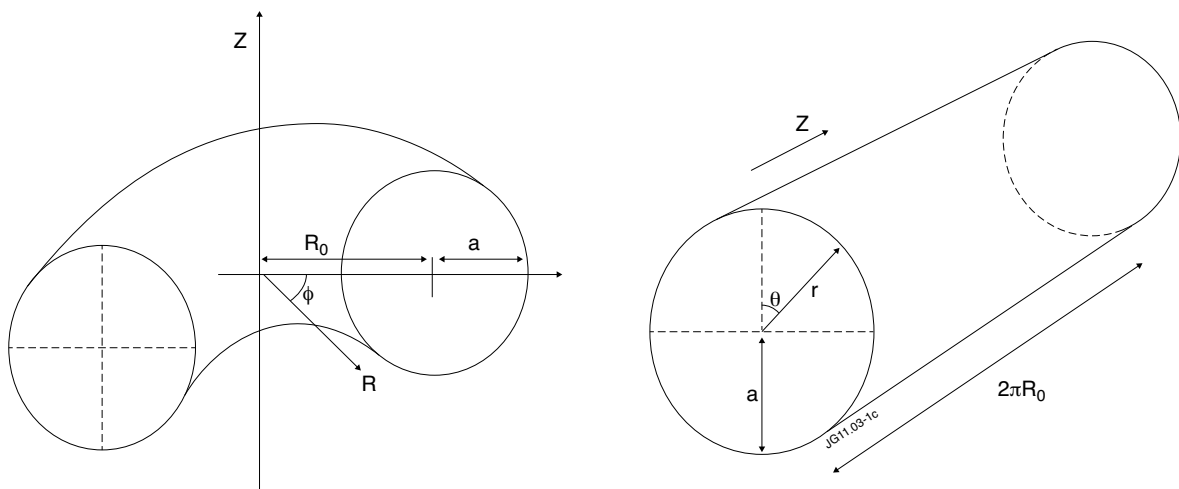


Figure 1: Tokamak toroidal geometry and its idealisation as a periodic cylinder.

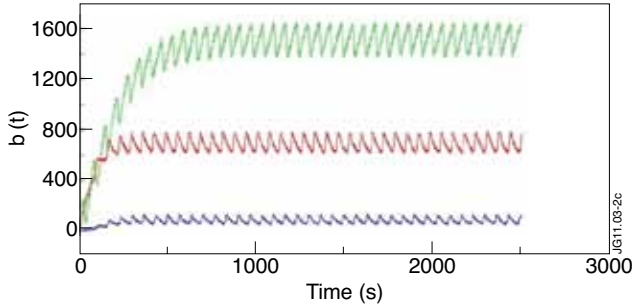


Figure. 2: Behaviour of b at three different major radii: 3.1m, 3.3m, 3.7 m. The parameters of equations (2) and (3) chosen to obtain these time evolutions are: Green curve $\delta = -0.4$ Red curve $\delta = -0.1$ Blue curve $\delta = 0$. For all the curves $\alpha = 1$, $\gamma = 1$, $m = 0.5$, $\beta = 10^{-3}$. The further addition of noise at the 10% level makes the plots very suggestive of experimental data.

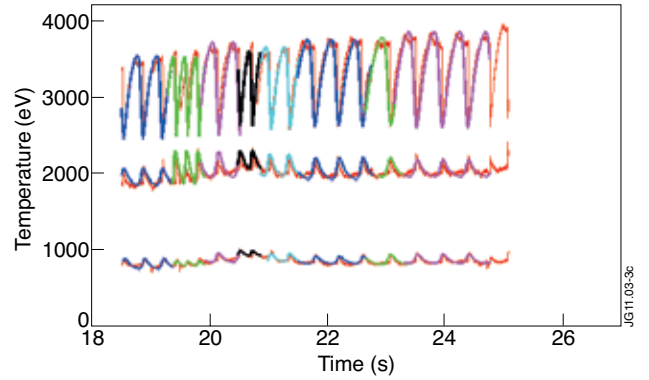


Figure 3: Fit of the time evolution of the electron temperature at three different major radii: 3.1m, 3.3m, 3.7m for JET Pulse No: 78765. The red curves are the experimental measurements. The other colours indicate the fits obtained using equations (2) and (3) adjusted for the different frequencies of the sawteeth in the various intervals. For clarity, to avoid overlap of the curves, 400keV have been subtracted from the absolute value of the temperature at radius 3.3m.

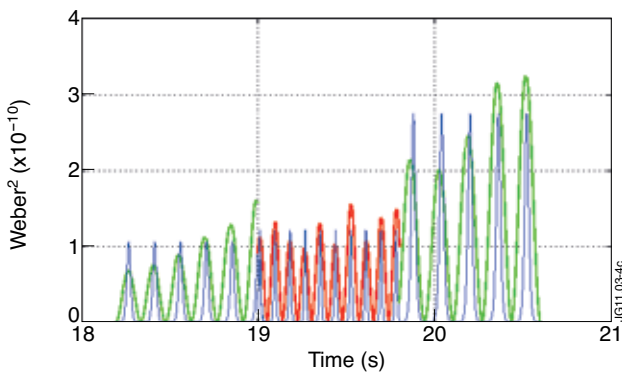


Figure 4. Comparison of a^2 and the square of the magnetic oscillations, measured by the pick-up coils for the same shot as figure 3. For clarity, the experimental signal, in blue, has been squared after removal of the offset and this explains the factor of 2 higher frequency with respect to figure 3.

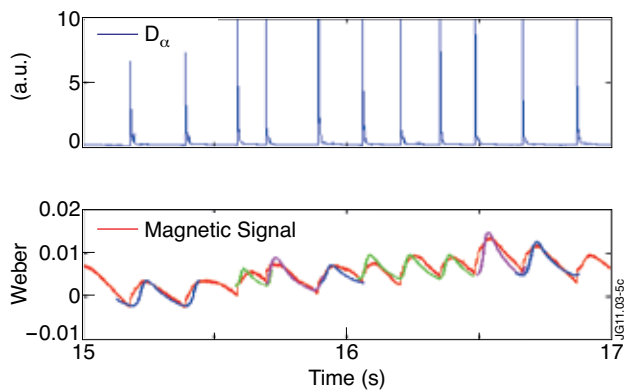


Figure 5. Fit of a series of ELMs in JET Pulse No: 73851. Top: D_α signal as a reference. Bottom: signal of a pick-up coil and its fit using equations (2) and (3). Since the system is not stationary, slightly different parameters have been used for the various time intervals (identified by different colours). The red curve represents the experimental measurement and the other colours the fitting curve $b(t)$.